Binding isotherms of surfactants used in detergent formulations to Bovine Serum Albumin

Helena Mateos[1*], Alessandra Valentini[2], Giuseppe Colafemmina[1], Sergio Murgia[3], Eric Robles[4], Anju Brooker[4], Gerardo Palazzo[1].

[1]*Department of Chemistry, University of Bari, and CSGI (Center for Colloid and Surface Science), via Orabona 4, 70125, Bari, Italy*

[2]*School of Chemical Engineering, University of Birmingham, B15 2TT, UK*

[3]*Department of Chemical and Geological Sciences, University of Cagliari, and CSGI (Center for Colloid and Surface Science), ss 554, bivio Sestu, 09042 Monserrato (CA), Italy*

[4]*Procter & Gamble Company, Newcastle Innovation Center, Newcastle-Upon-Tyne NE12 9TS, UK*

https://doi.org/10.1016/j.colsurfa.2020.124801

Abstract

Protein-surfactant interactions are the focus of extensive research due to their many applications in food technology and detergent industry. In this work, we investigate the interaction between bovine serum albumin (BSA) and five relevant surfactants to the cleaning industry, which differ in head group charge, namely: sodium alkyl ether sulphate (C_{12}-C_{14} AE_3S), Cocoamidopropyl amine-oxide (CapAO) , alkyl dimethyl amine oxide ($C_{12}C_{14}AO$), octaethylene glycol monodecyl ether ($C_{10}EO_8$) and didecyldimethylammonium chloride (DDAC). The results collected with fluorescence emission spectroscopy highlight zwitterionic and nonionic surfactants have the lowest affinity for the protein, as their interaction does not result in protein denaturation. Instead, higher and mutually close binding constants are found for AE_3S (anionic) and DDAC (cationic) due to the presence of electrostatic interactions between the surfactant heads and the charged residues of BSA. AE_3S leads to irreversible protein unfolding. The case of DDAC is more complex and has been studied through a combination of fluorescence, DLS, PGSE-NMR and zeta-potential measurements. At low concentration DDAC binding neutralizes negatively charged residues present in BSA, causing a reversible flocculation of BSA after the isoelectric point (23 DDAC molecules per protein). Further DDAC adsorption, at 70 DDAC molecules per protein, leads to an excess of positive charge on the protein which restores electrostatic repulsions between BSA-surfactant complexes.

1. Introduction

Proteins and surfactants tend to interact since they are both amphiphilic molecules.[1–8] Surfactants can frequently lead to protein denaturation in a process that might result in irreversible conformational changes.[9,10] The applications of protein-surfactant interactions lay particularly on food technology, detergent formulations and personal hygiene products.[11–17]

For example, the formation of complexes between surfactants and proteins in the dirt is the primary mechanism for proteic dirt removal,[18] which is essential to the detergency process. Proteins are often a fundamental component of what detergents are expected to clean (humans included). Proteins of the hair or certain fabrics, like wool, are routinely in contact with surfactants and some detergent-skin irritation issues are related to the interaction of the stratum corneum proteins with surfactants.[19–21] Besides, many detergent formulations contain proteolytic and lipolytic enzymes.[22]

The interactions between surfactants and proteins is also fundamental for the scientific research: the extraction and the purification of membrane proteins is possible only thanks to suitable non-ionic surfactants,[23,24] and gel electrophoresis uses anionic surfactants for the determination of proteins' molecular weights. In the preliminary

treatment to an SDS-PAGE (sodium dodecyl sulphate-polyacrylamide gel electrophoresis) run, the protein is fully denatured by exposure at high temperatures in the presence of the anionic surfactant SDS.[10] The thermal denaturation process is ruled by the balance between folded and unfolded forms, influenced by the presence of surfactants as well as by pH, temperature or ionic strength.

The present study is a pooled description of the effect of conventional surfactants with different headgroups, all relevant for industry, on a protein. We chose BSA as our model protein since it has two tryptophan (Trp) residues, which are intrinsically fluorescent and can be an indication of protein denaturation. On the other hand, we chose five surfactants pertaining to four main groups: anionic, zwitterionic, nonionic and cationic (see Table **1**). We used fluorescence spectroscopy at room temperature to investigate the effect of surfactant concentration on the protein when the molecules are free to interact in solution. Changes in size and charge have been probed in parallel by DLS, and laser Doppler electrophoresis (LDE). Also, by PGSE-NMR was used on selected samples to measure the fraction of surfactant bound to protein.

2. Material and methods

BSA protein (purity > 98%) was purchased from Sigma-Aldrich and used without any further purification. The anionic surfactant was sodium alkyl ether sulphate with three degrees of ethoxylation and a mixture of 12 and 14 carbon units in alkyl chain length (C_{12}-C_{14} AE3S, supplied by Stepan as a 75% paste). Two amine oxide zwitterionic surfactants; Cocoamidopropyl amine-oxide (CapAO, supplied as 40% solution in water from BASF) and alkyl dimethyl amine oxide (C_{12}-C_{14}AO, supplied as 32% solution in water). Finally, the neutral octaethylene glycol monodecyl ether ($C_{10}EO_8$, supplied by Sasol with a purity grade 95%) and cationic didecyldimethylammonium chloride (DDAC, supplied by Lonza as a 72% solution in water).

2.1 BSA isothermal titration with surfactants

All BSA and surfactant samples were prepared in phosphate-buffered saline (PBS, 0.01 M phosphate buffer, 0.0027 M potassium chloride and 0.137 M sodium chloride, pH 7.4, at 25°C) except for the case of the surfactant DDAC, for which samples were prepared in deionized water to avoid phosphate-quaternary ammonium interactions. The pH of the DDAC samples was 6.5 at 25°C .

The steady-state fluorescence spectra were collected using a Varian Cary Eclipse fluorescence spectrophotometer (Agilent Technologies) in 1 cm path quartz cuvettes. The excitation wavelength used to trigger the Trp response was 280 nm and the emission spectra in the range 300 nm -500 nm where collected. The detector was protected by a filter that removes light at wavelength below 300 nm. The excitation source was a xenon flash lamp. Before each titration the excitation and emission slits where adjusted in order to have a value of the emission at 345 nm above 200 a.u. for the solution of BSA without any surfactants (typical values are 2.5 nm).

Nanosizer ZS (Malvern instruments) was used for the determination of the zeta potential (laser Doppler Electrophoresis EDL) and of the size distribution (Dynamic Light Scattering, DLS) of particles in solution. DLS measurements were performed in backscattering at fixed detector angle of 173° (NIBS™), while the zeta potential measurements were performed using forward scattering (13°) setup in capillary cells. DLS data were collected leaving the instrument free to optimize the instrumental parameters (attenuator, optics position and number of runs). Usually the time autocorrelation function (ACF) of scattered light intensity was the average of 10-12 consecutive runs of 10 s each. The size distribution by intensity of scattered light was recovered, using the software implemented by the manufacturer, by taking the inverse Laplace transform of the ACF and subsequent application of Stokes-Einstein equation, assuming the viscosity of the water solution at 25°C.

2.2. NMR Measurements

^{1}H NMR measurements were carried out in ^2H_2O (D_2O) at 25 °C through a Bruker Avance 300 MHz (7.05 T) spectrometer at the operating frequencies of 300.131, and 46.072 MHz, respectively. A standard BVT 3000 variable temperature control unit with an accuracy of ±0.5 °C was used. Self-diffusion coefficients were determined using a Bruker DIFF30 probe supplied by a Bruker Great 1/40 amplifier that can generate field gradients up to 1.2 T m^{-1}.

The pulse-gradient stimulated echo (PGSTE) sequence was used. Self-diffusion coefficients were obtained by varying the gradient strength (g) while keeping the gradient pulse length (δ) and the gradient pulse intervals constant within each experimental run. The data were fitted according to the Stejskal- Tanner equation:

$$\frac{I}{I_0} = \exp(-Dq^2t) \quad (1)$$

Where I and I_0 are the signal intensities in the presence and absence of the applied field gradient, respectively. Also, $q = \gamma g\delta$ is the so-called scattering vector (γ being the gyromagnetic ratio of the observed nucleus), $t = (\Delta - \delta/3)$ is the diffusion time, Δ is the delay time between the encoding and decoding gradients, and D is the self-diffusion coefficient to be extracted.[25] Errors on the self-diffusion coefficients were estimated at around 2% based on repeated measurements.

3. Theory and calculation

Bovine serum albumin (BSA) is a water-soluble protein with a molecular weight of 66.5 kDa. The structure of BSA consists of three globular, homologous domains comprised of six α-helices. The polypeptide chain of BSA is formed by 583 amino acids, from which, only two are tryptophan residues. Trp-134 lies in a hydrophilic environment near the surface in domain I. Tryptophan has a fluorescent indole group that is very sensitive to the polarity of the environment, thus evidencing the location of tryptophan in the protein. When the protein unfolds, tryptophan groups are exposed from a hydrophobic environment to the polar, aqueous phase, and the emission spectrum decreases and shifts to lower energies (higher wavelength).[26–28] Trp-212 is located in an inner, hydrophobic environment in the protein, and contributes more to the fluorescence intensity.[29,30] During the thermal denaturation process of a protein, hydrophobic interactions are strengthened while the hydrogen bonds are weakened and finally broken as heating increases.[31,32]

The unfolding of proteins usually causes a displacement of the emission maximum towards higher wavelengths as the tryptophan residue is exposed to the polar environment of water. However, upon addition of surfactants, the maximum emission might shift towards lower wavelengths instead.[8,33,34] This behaviour indicates that the tryptophan environment remains apolar and therefore, BSA only undergoes partial denaturation without complete loss of its secondary structure.[35]

The denaturation power of surfactants depends mostly on the nature of their head groups. Neutral surfactants usually do not denature proteins (that is the reason why they are used to purify functional membrane proteins), while ionic ones do, typically at very low concentrations. The formation of protein-surfactant complexes undergoes a range of multistep equilibria as the surfactant monomers S interact with the protein P to both native and denatured states:[36–38]

$$\begin{aligned} P + S &\leftrightarrow PS \\ PS + S &\leftrightarrow PS_2 \\ PS_{n-1} + S &\leftrightarrow PS_n \end{aligned} \quad (2)$$

The total concentration of protein-bound to surfactant $[P \cdot S_n]$, is:

$$[P \cdot S_n] = \sum_{J=1}^{J_{max}} [P \cdot S_J] \quad (3)$$

Where J_{max} is the maximum number of surfactant molecules that can bind to a protein. By probing the tryptophan emission, we cannot distinguish between proteins bound to a different number of surfactants (say between $[P{\cdot}S_1]$ and $[P{\cdot}S_3]$) and therefore $[P \cdot S_n]$ is the only experimentally accessible parameter.

The fraction of protein-bound to surfactant (α) is given as the concentration of bound protein divided by the total protein concentration:

$$\alpha = \frac{[P \cdot S_n]}{[P_T]} \tag{4}$$

The challenge in managing the chain of reactions described in scheme 1 is due to the heterogeneity of the binding processes. A protein is a large macromolecule with several potential binding sites. Thus, depending on the nature of protein and surfactant, one expects to observe an assortment of behaviours, differing in the degree of cooperativity, ranging from totally independent binding sites to a stoichiometric binding.

In the case where the *n* binding sites have all the same affinity for the surfactant and assuming no interaction between surfactant molecules, one retrieves the well-known Langmuir's isotherm:

$$\alpha = \frac{K[S]}{1 + K[S]} \tag{5}$$

Where K denotes the Langmuir's (binding) constant.

The opposite situation of extreme cooperativity is where a protein binds exactly *n* surfactant molecule in a single step so that the process $P+nS \leftrightarrow P{\cdot}S_n$ is described by the equilibrium constant.

$$K_n = \frac{[P \cdot S_n]}{[S]^n[P]} \tag{6}$$

The real situation is somewhere between these two extremes: at the beginning, the surfactant binds to roughly equivalent binding sites but as the unfolding progresses it exposes internal regions of the protein to interact with the surfactant thus enhancing the binding. In order to account for such a cooperativity effect, the Hill formalism can be used. According to such a model the Hill's coefficient n_H is used in equation **6** instead of *n*. The parameter n_H quantifies the degree of cooperativity: $n_H > 1$ positively cooperative binding; $n_H = 1$ noncooperative (completely independent) binding; $n_H < 1$ negatively cooperative binding. According to Hill's model, the fraction of protein-bound to surfactant is:

$$\alpha = \frac{K_H[S]^{n_H}}{1 + K_H[S]^{n_H}} \tag{7}$$

Where K_H in this equation denotes the overall binding constant with dimensions of M^{-n_H}, to enable an easy comparison of the data, we will discuss the affinity in terms of the average equilibrium constant of the elementary binding step $K = \sqrt[n_H]{K_H}$ which has dimensions of M^{-1}.

4. Results and discussion

4.1 Overview of BSA- surfactants interactions

Fluorescence spectroscopy has been previously used to monitor the changes in the conformation of BSA upon addition of archetype surfactants like SDS and then, more recently with the addition of new promising amphihilic molecules.[8,33,39,40] However, a detailed study on the interaction between BSA and industrial surfactants is much less common. Here, we have performed isothermal titrations of BSA at constant 1mg/mL by adding surfactants ranging in concentrations from 0.05 to 70 mM.

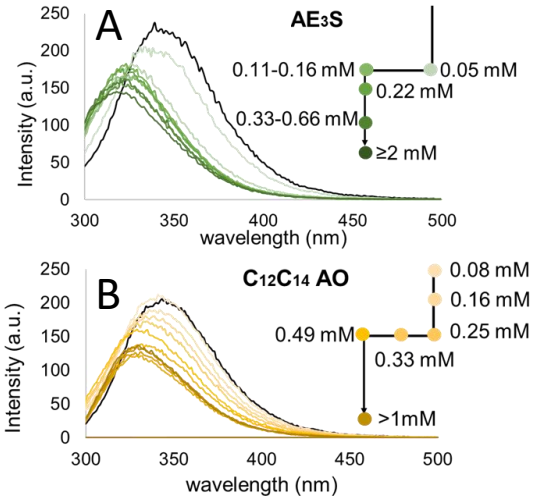

Figure 1. Fluorescence emission spectra of BSA (black line) in PBS at pH 7.4, λ_{exc} = 280 nm, in the presence of increasing concentrations of surfactants (coloured lines); The arrows indicate the sequence of maximum intensity changes upon surfactant concentration. A) AE_3S. B) $C_{12}C_{14}AO$

Native BSA has a broad emission spectrum with a maximum around 345 nm. At high surfactant concentration, the fluorescence spectrum is quenched, shifting its maximum to around 320 nm. As previously reported in literature in the case of the anionic surfactant SDS,[35],[41] the shift is discontinuous, and, therefore, it is possible to discern the presence of at least three species. A BSA-surfactant complex is found at intermediate SDS concentrations ($I_{max} at\ 330\ nm$) where the protein still retains its native conformation. Further addition of SDS results in a maximum quenched spectrum, which has been identified with the (partially) denatured protein.

Fig. 1A shows the fluorescence spectra of BSA upon loading with anionic AE_3S, which provokes very similar alterations to those reported for SDS. Otherwise, the effect of a zwitterionic amine-oxide on BSA is shown in fig. 1B. Both in the cases of the two zwitterionic amine-oxide and the non-ionic (ethoxylate) surfactants, the maximum of fluorescence at high surfactant concentration was found around 330 nm. This indicates that despite the surfactants interact with BSA, they do not fully denature the protein even at high concentrations.

The cationic double-tailed surfactant DDAC, showed a peculiar behaviour in the presence of BSA: adding DDAC to the solution produced a first drop in the intrinsic BSA fluorescence. However, further addition of surfactant caused an increase of fluorescence intensity (without any shift in the peak position).

In order to compare the adsorption of different surfactants to the protein, we normalized the point of maximum difference between the emission in the native and denatured state (330 nm) to the fluorescence of native BSA. Representative results of AE_3S, CapAO, AO and $C_{10}EO_8$ are shown in Fig. 2, while the results obtained for DDAC are shown in Fig.3.

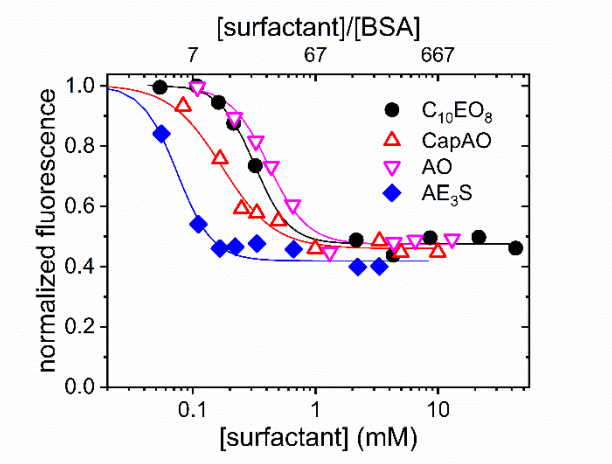

Fig. 2. Dependence of the normalised fluorescence of BSA (1 mg/mL) upon addition of surfactants; lower abscissa is the surfactant concentration and upper abscissa is the mole ratio surfactant/BSA. Lines are the best-fit according to eqs.7 and 8 (the best-fit parameters are listed in Table 1).

AE_3S produces the maximum quenching (residual fluorescence ~ 40%) at a very low concentration (~ 10 surfactant/BSA mole ratio). According to the position of the fluorescence peak (Fig. 1A) the species at high AE_3S concentration corresponds to partially unfolded BSA.

The zwitterionic and non-ionic surfactants, instead, require ~ 70 surfactant molecules per BSA to reach saturation. The fluorescence quenching, however, corresponds to a higher residual fluorescence (~ 50%). According to the position of the fluorescence peak (see for example Fig. 1B) the species at high surfactant concentration corresponds to BSA containing bound surfactant molecules altough not yet unfolded.

The surfactants affinity for BSA (Fig. 2) was evaluated according to the "all or none" model which assumes the protein can only exist either in the native ($F_0 = 1$) or in the final state (with a normalized fluorescence that corresponds to the lowest value found at high surfactant concentration, F_{min}). Intermediate values of normalized fluorescence (F_{norm}) were attributed to the coexistence of these two states. Therefore, data in Fig. 2 were fitted to the following equation:

$$F_{norm} = (1 - \alpha)F_0 + \alpha F_{min} \qquad (8)$$

Where α is the fraction of protein-bound to surfactant, and it is supposed to obey the Hill's equation (eq. 7). The curves in Fig. 2 represent the prediction of such a fitting procedure, and the best-fit parameters are listed in Table 1.

Table 1. Binding constants and Hill's coefficients (eq. 7) calculated for each surfactant-BSA studied case, together with the CMC values of the surfactants. The calculated values of K and n_H are means ± standard deviation obtained from the fittings in Fig. 2.[a]

CLASS	SURFACTANT	CMC /mM	K /mM^{-1}	n_H
ANIONIC	$C_{12}C_{14}$ 3-Ethoxy sulphate (AE_3S)	0.8	13.5±1.5	3.0±0.7
ZWITTERIONIC	Cocoamidopropyl Amine-oxide (CapAO)	2.2	6±1	2.0±0.4
	C_{12}-C_{14} Amine-Oxide (AO)	1.7	2.4±0.2	2.7±0.5
NON-IONIC	C_{10} 8-Ethoxy ($C_{10}EO_8$)	0.9	3.13±0.01	3.1±0.5
CATIONIC	Didecyldimethylammonium chloride (DDAC)	0.5	10±2	Langmuir model (n_H≡0)

According to the analysis of the binding isotherms in Fig. 2, the scale of affinity for BSA is AE_3S >> CapAO >> $C_{10}EO_8$ ≈ AO. The anionic surfactant shows the highest affinity for the protein. The binding constant is close to that reported for the anionic surfactant SDS (10 mM^{-1}) and this fact, considering the similar size of the hydrophobic tails of the surfactant explored, suggests that electrostatic attraction for basic protein residues is the main contribution to such high affinity.

Concerning the degree of cooperativity, quantified by the Hill's coefficient n_H, AE_3S, $C_{10}EO_8$ and AO are mutually close with $n_H \approx 3$, while CapAO has a slightly lower value.

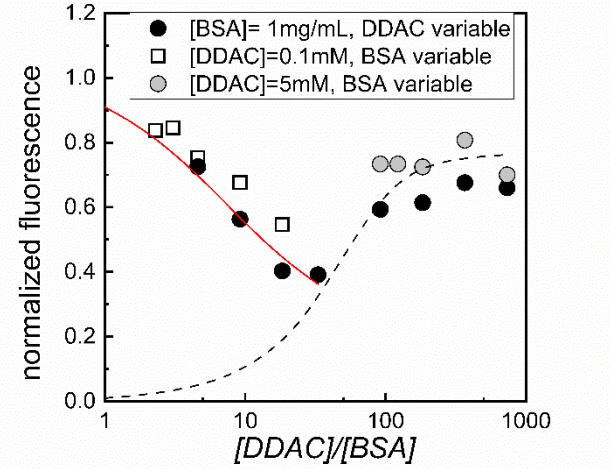

Fig.3. Normalised intensity of BSA (1mg/mL) upon addition of DDAC (black dots) as a function of the ratio [DDAC]/[BSA], together with the experiments at increasing BSA and constant surfactant concentration (0.1 mM DDAC, empty squares and 5 mM DDAC, grey dots). The red curve is the best fit to eqs. 5 and 8 for [DDAC]/[BSA]< 23 (K=10±2 mM^{-1}). The dashed line is the prediction according to eqs. 8 and 11 with the same binding constant and n=70; in such a case considering the resuspension process it was assumed F_0=0.

The effect of DDAC addition on the intrinsic BSA fluorescence is shown in Fig. 3 as black dots. As stated above, the behaviour of DDAC is unusual. Loading a BSA solution with DDAC produces an initial decrease of fluorescence, reducing the quantum yield to the 40% of initial value while leaving constant the position of the peak. Further addition of DDAC results in a fluorescence increase, up to an 80% quantum yield from the initial value. This behaviour was previously reported for the addition of cetyltrimethylammonium chloride (CTAC) to BSA by Gelamo et al. although it was not rationalised [35]. However, other studies using similar trimethylammonium cationic surfactants on BSA do not report this behavior but that of typical anionic surfactants instead.[7,33]

The position of the fluorescence maximum remains fixed at 345 nm suggesting negligible changes close to the tryptophan molecules and indicating there are other processes taking place in this system different from the folding/unfolding equilibria.

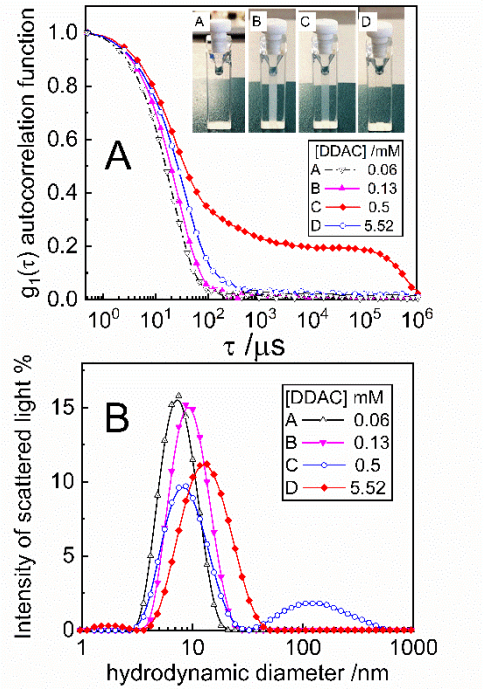

Fig. 4. Dynamic light scattering study of the BSA-DDAC system. A) autocorrelation function and B) intensity-weighted size distribution functions. [BSA]= 1 mg/mL.

Visual inspection of the samples immediately after preparation (see the picture in Fig. 4A) suggests that such non-monotonic behaviour mainly reflects the solubility of the protein-surfactant complex. Indeed, loading a 1 mg/mL BSA solution with DDAC results in a turbid sample for concentration above 0.1 mM (~ 10 [DDAC]/[BSA]). This concentration corresponds to the start of a more pronounced decline in fluorescence, suggesting a fraction of the fluorescence drop is caused by a combination of light scattering and of BSA precipitation, reducing the BSA concentration in solution. Further addition of surfactant provokes a turbidity increase until a given concentration, that in the case of BSA 1 mg/mL is close to the CMC of DDAC = 0.5 mM. Loading with surfactant above this critical value results in a recovery of the fluorescence intensity, and the solutions returns transparent.

Fig. 4 shows the results of DLS measurements performed on equilibrated samples below and above the critical value. At lower concentration, the DLS autocorrelation function is monomodal (Fig. 4A) and is accounted for size distribution (Fig. 4B) centred at a hydrodynamic diameter of 9 nm, that corresponds to the size of the native BSA. At [DDAC] = 0.5 mM the DLS autocorrelation function is markedly poly-modal with a "tail" at longer correlation times that is diagnostic of large aggregates (Fig. 4A). Accordingly, the size distribution reveals the coexistence of small particles with the size of BSA and large aggregates (Fig. 4B). At large DDAC concentration, the DLS autocorrelation function returns monomodal, but the corresponding hydrodynamic diameter is larger (11 nm) than that of native BSA. Such an increase in the hydrodynamic size takes place without any change in the position of the BSA fluorescence, which remains fixed at the value attributed to BSA bound to surfactants but still folded. It therefore cannot be explained by swelling of a denaturated protein. This behaviour could be rationalised as due to the formation of a surfactant layer around the protein, since the size increment (+2 nm) is comparable to the length of the surfactant.

The fact that the minimum in fluorescence (and the corresponding BSA aggregation) takes place close to the CMC of DDAC is fortuitous. The DDAC-BSA interaction seems to be governed by the relative concentrations instead of the presence (or absence) of micelles. Indeed, it is possible to tune the fluorescence of BSA above and at the CMC, at constant [DDAC] by regulating the mole ratio between surfactant and protein (R = [DDAC]/[BSA]). This is shown in Fig. 3 where the experiments at fixed BSA and variable surfactant (black dots) are compared with experiments at fixed surfactant and variable BSA (open squares and grey circles).

Interestingly, in the case of experiments at low surfactant concentration (0.14 mM; empty squares in Fig. 5) it is possible to increase the normalized fluorescence of the protein back to the quantum yield of the native protein by adding BSA, and, therefore, decreasing the surfactant/BSA ratio.

BSA at pH> 4.5 bears a negative charge [42] (we have measured a ζ-potential of – 8 mV in PBS and -15 mV in water). This suggest an electrostatic driving force. Indeed the ζ-potential measurements (Fig. 5), performed at constant [DDAC] and increasing amounts of BSA, indicate that binding of DDAC molecules screen the negative charges on BSA until an isoelectric point is reached at a [DDAC]/[BSA] ratio close to 23. This leads to a reversible aggregation of the protein. Further addition of DDAC ([DDAC]/[BSA]>70) restores the electrostatic repulsive potential that allows the resuspension of BSA. At this point, the ζ-potential is strongly positive, demonstrating we are dealing with the formation of protein surfactant complexes. A recent study on the interaction between DDAB and BSA has been reported by Papagiannopoulos [43] for 1000 < [DDAC]/[BSA] < 10000. They report a constant apparent molecular weight of the system in the range of concentrations explored, which is aligned with our observations.

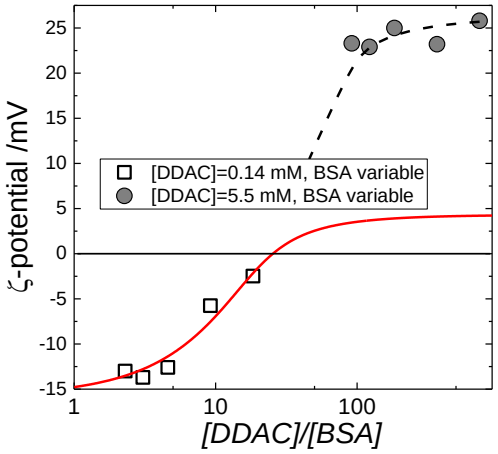

Fig. 5. ζ-Potential measurements of samples with constant DDAC (0.14mM – empty squares and 5.5mM grey dots) at increasing BSA concentrations. The curves are the predictions according to eqs. 8 and 11 with K=10 mM^{-1}. Red curve n= 23 F_0= -15 mV F_{min}= +1.5 mV; dashed line i n=70; in such a case, considering the resuspension of a neutral complex, F_0= 0 mV F_{min}= +25 mV.

Assuming the decrease in fluorescence is proportional to the fraction of protein bound to DDAC, the region at [DDAC]/[BSA] < 23 can be described using a Langmuir isotherm with a binding constant of K= 10 mM^{-1} (red curve in Fig. 3). In such a case, it is not necessary to rely on the Hill's model since, within the experimental uncertainty, n_H =1.

As long as our experimental observable is the fraction of BSA-surfactant complex evaluated with respect of the protein, it is impossible to obtain information on the number of surfactants involved in the different steps of binding. This is because the fraction of binding/adsorption sites occupied by a surfactant is indistinguishable from the fraction of bound protein:

$$\frac{n[P{\cdot}S_n]}{n[P_T]} = \frac{[P{\cdot}S_n]}{[P_T]} = \alpha \qquad (9)$$

In the case of a protein with n binding sites that obey the equilibria of scheme 1, with the same affinity (Langmuir isotherm) the presence of multiple binding sites can be accounted for by considering the initial (n[P$_T$]) and the actual (n[P]) concentration of empty binding sites.

If we denote the initial surfactant concentration as [S$_T$], then the free surfactant concentration [S] can be written as [S]= [S$_T$]-α n[P$_T$] and equation 4 becomes:

$$\alpha = \frac{K([S_T]-\alpha n[P_T])}{1+K([S_T]-\alpha n[P_T])} \qquad (10)$$

Which can be rewritten in terms of the ratio R=*[DDAC]/[BSA]*= [S$_T$]/[P$_T$] as

$$\alpha^2 - \alpha\left(\frac{R}{Kn[P_T]} + \frac{R}{n} + 1\right) + \frac{R}{n} = 0 \qquad (11)$$

That has as solutions:

$$\alpha = \frac{\left(\frac{R}{Kn[P_T]}+\frac{R}{n}+1\right)-\sqrt{\left(\frac{R}{Kn[P_T]}+\frac{R}{n}+1\right)^2-4\frac{R}{n}}}{2} \qquad (12)$$

However, in eq. 12 the parameters K (binding constant) and n (number of binding sites on a protein) are so strongly correlated that they cannot be resolved in a best-fit procedure. To obtain an estimate for *n* we were forced to resort to a technique that probes the *fraction of bound surfactant*.

This kind of partition equilibria between bound and free ligand can be profitably investigated by means of PGSE-NMR, a technique that permits to measure the molecular self-diffusion coefficients.[42,44]

Being an NMR technique, it suffers of low sensibility compared with fluorescence and therefore we limited the study to a fixed high surfactant concentration, [DDAC]= 5.52 mM and variable BSA concentration in order to explore the range 90< [DDAC]/[BSA]<130. Using PGSE-NMR it has been possible to determine the diffusion coefficient of DDAC in the presence and absence of BSA together with the diffusion coefficient of the surfactant monomer. The combination of low concentration and short T_2 relaxation time does not allow the measurement of the BSA diffusion coefficient by means of NMR but it was evaluated from DLS instead. The experimental data are summarized in Fig. 6.

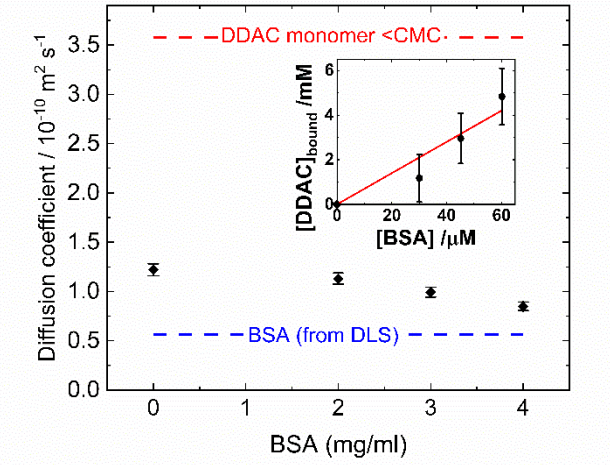

Fig. 6. Diffusion coefficient of the DDAC/BSA system at constant DDAC (5.5 mM) and variable BSA. Inset: evolution of the concentration of DDAC bound to the protein (see text for details).

The diffusion coefficient of the free DDAC monomer in solution D_{free}=(3.2±0.2)x10^{-10} m^{2}s^{-1}, is much higher than that of BSA D_{BSA}=(0.57±0.03)x10^{-10} m^{2}s^{-1}. Above the CMC (and no protein present) a fraction of the surfactant is involved in the micelles resulting in a lower self-diffusion coefficient of (1.22 ± 0.06)x10^{-10} m^{2}s^{-1}. Such an observed value (D_{obs}) corresponds to the population average of the diffusion coefficients of monomeric surfactant and of micellized surfactant according to:

$$D_{obs} = P_{free}D_{free} + P_{mic}D_{mic} \qquad (13)$$

Where D_{mic} is the diffusion coefficient of the micelle and $P_{free} = \frac{CMC}{[S_T]}$ and $P_{mic} = \frac{CMC-[S_T]}{[S_T]}$ are the fraction of monomeric and micellized surfactant, respectively.

Knowing P_{free} and P_{mic} from the composition and from the CMC value it is possible to evaluate D_{mic}=(1.00±0.05)x10^{-10} m^{2}s^{-1}.

In the case of the BSA-containing samples, the presence of a fraction of surfactant bound to the slow diffusing BSA accounts for the 30% decrease in the observed diffusion coefficient in the presence of 4 mg/mL of BSA (see Fig. 6).

Interestingly, analogous experiments performed on the non-ionic surfactant $C_{10}EO_8$ do not reveal any change in its diffusion coefficient indicating that the fraction of surfactant bound to the BSA is negligible (data not shown).

In the case in which the surfactant exists in three mutual fast exchange forms; monomer, constituent of a micelle, and bound to BSA (with mole fractions P_{free}, P_{mic}, and P_{bound}, respectively) the generalization of eq.13 is straightforward:[45]

$$D_{obs} = P_{free}D_{free} + P_{mic}D_{mic} + P_{bound}D_{BSA} \quad (14)$$

In the above equation the diffusion coefficients D_{free}, D_{mic}, and D_{BSA} are known and constant (the concentration of DDAC and BSA is so low that we can neglect any obstruction effect to the diffusion). Assuming that the CMC is unaffected by the presence of the protein ($P_{free} = \frac{CMC}{[S_T]}$), the constraint 1= P_{free}+P_{mic} + P_{bound} allows to calculate the fraction of surfactant bound to BSA as:

$$P_{bound} = \frac{D_{obs} - P_{free}D_{free} - (1 - P_{free})D_{mic}}{D_{BSA} - D_{mic}} \quad (15)$$

It should be noted that the outcome of the above equation depends critically on the differences between diffusion constants. Accordingly, although the uncertainty on the single diffusion coefficient is below 5%, the error associated to the P_{bound} value grows dramatically as D_{free} and D_{obs} values approach. For this reason, it was not possible to probe the bound surfactant for BSA concentrations lower than 2 mg/mL. At constant [DDAC], the fraction of surfactant bound to the protein ($[BSA]_{bound}$) increases linearly with the protein content with a slope that corresponds to 70 surfactant molecules per BSA molecule, as shown in the inset of Fig. 11. The line in the inset corresponds to $[BSA]_{bound} = n\alpha[BSA]$ where α is given by eq. 12 with a fixed binding constant K=10 mM and n=70±8. It should be noted that due to the high surfactant and protein concentration the prediction of eq. 12 is indistinguishable from a straight line.

According to the PGSE-NMR results, at surfactant concentration of 5 mM, BSA is saturated by roughly 70 surfactant molecules. From ζ-potential measurements (Fig. 5) we know that such a situation corresponds to a soluble cationic complex between surfactants and protein. Accordingly, we have rationalized the peptization (deflocculation and re-solubilisation) caught by the pictures of Fig. 4A and probed by the raise in fluorescence occurring for [DDAC]/[BSA] above 23 of Fig. 3 as the formation of the saturated complex made by one BSA and 70 DDAC. The dashed line in Fig. 3 is the prediction for eq. 13 with n= 70 and K= 10 mM. and is in very good agreement with the experimental data.

5. Conclusions

In this work we have compared the interaction behaviour of BSA and a range of widely used surfactants in detergent formulations through a combinational study of fluorescence spectroscopy, DLS, ζ-potential measurements and PGSE-NMR.

Zwitterionic (CapAO and AO) and non-ionic ($C_{10}EO_8$) surfactants have the lowest affinity for the protein and their binding does not results in a denaturation of the protein even at high concentrations. These mild surfactants bind cooperatively to a small number of hydrophobic sites without perturbing the protein conformation.

The binding constants of charged surfactants (DDAC and AE_3S) are higher and mutually close (around 10 mM^{-1}). This indicates the electrostatic interaction between surfactant polar heads and charged residues of the protein plays an important role in the affinity for the protein, independently from the charge on the surfactant. The nature of the surfactant charge becomes fundamental in ruling the fate of the protein once the binding has occurred. In the case of the anionic surfactant, the conformation of the BSA-AE_3S complex evolves towards an unfolded state likely due to a swelling caused by the mutual repulsion among bound surfactants. On the other hand, the binding of the cationic DDAC on the protein follows a particular behaviour. At pH > 4.5, BSA has an excess of negative charged residues and the initial binding of DDAC results in a charge neutralization avoiding the intra-protein repulsive interactions. The isoelectric point is reached at a value of 23 DDAC molecules per protein leading to a flocculation of the protein-surfactant complex due to a screening of the inter-protein repulsive interactions. Further adsorption of DDAC restores a net (positive) charge on the protein, favouring the peptization of the proteins. It is interesting to note that other similar quaternary ammonium surfactants do not interact with BSA in the same manner. [7,33] In this

perspective, the present investigation improves the understanding of cationic surfactant-protein interactions and, on the applicative ground, supports the design of future detergents formulations for pharmaceutical, drug delivery or detergent industry.

Funding

This work is funded by the European Union's Horizon 2020 research innovation programme under grant agreement No. 722871 in the scope of the Marie Sklodowska-Curie Action ITN BioClean. Partial financial support by the Center for Colloid and Surface Science (CSGI) is acknowledged.

References

[1] T.W. Randolph, L.S. Jones, Surfactant-Protein Interactions, in: Carpent. J.F., Manning M.C. Ration. Des. Stable Protein Formul. Pharm. Biotechnol., Springer, Boston, MA, 2002: pp. 159–175. doi:10.1007/978-1-4615-0557-0_7.

[2] P. Linse, N. Källrot, Polymer Adsorption from Bulk Solution onto Planar Surfaces: Effect of Polymer Flexibility and Surface Attraction in Good Solvent, Macromolecules. 43 (2010) 2054–2068. doi:10.1021/ma902338m.

[3] M.N. Jones, Surfactant interactions with biomembranes and proteins, Chem. Soc. Rev. 21 (1992) 127–136. doi:10.1039/CS9922100127.

[4] A. Al-Ani, A. Boden, M. Al Kobaisi, H. Pingle, P.-Y.Y. Wang, P. Kingshott, The influence of PEG-thiol derivatives on controlling cellular and bacterial interactions with gold surfaces, Appl. Surf. Sci. 462 (2018) 980–990. doi:10.1016/j.apsusc.2018.08.136.

[5] Y. Li, J.S. Lee, Staring at protein-surfactant interactions: Fundamental approaches and comparative evaluation of their combinations - A review, Anal. Chim. Acta. (2019). doi:10.1016/j.aca.2019.02.024.

[6] V. Sharma, P. Cantero-lópez, O. Yañez-Osses, C. Rojas-Fuentes D, A. Kumar, C. Rojas-fuentes, A. Kumar, C. Rojas-Fuentes D, A. Kumar, C. Rojas-fuentes, A. Kumar, Influence of BSA on micelle formation of SDBS and CPC: An experimental-theoretical approach of its binding properties, J. Mol. Liq. 271 (2018) 443–451. doi:10.1016/j.molliq.2018.09.003.

[7] T. Janek, P. Czeleń, E.J. Gudiña, L.R. Rodrigues, Ż. Czyżnikowska, Biomolecular interactions of lysosomotropic surfactants with cytochrome c and its effect on the protein conformation: A biophysical approach, Int. J. Biol. Macromol. 126 (2019) 1177–1185. doi:10.1016/j.ijbiomac.2019.01.024.

[8] T. Janek, L.R. Rodrigues, Ż. Czyżnikowska, Ż. Czy, Study of metal-lipopeptide complexes and their self-assembly behavior, micelle formation, interaction with bovine serum albumin and biological properties, J. Mol. Liq. 268 (2018) 743–753. doi:10.1016/j.molliq.2018.07.118.

[9] S. Magdassi, Surface Activity of Proteins: Chemical and Physicochemical Modifications, 1996. doi:10.1002/food.19970410415.

[10] D. Otzen, Protein-surfactant interactions: A tale of many states, Biochim. Biophys. Acta - Proteins Proteomics. 1814 (2011) 562–591. doi:10.1016/j.bbapap.2011.03.003.

[11] U.K. Laemmli, Cleavage of structural proteins during the assembly of the head of bacteriophage T4, Nature. 227 (1970) 680–685. doi:10.1038/227680a0.

[12] J. Jiang, Y. Jin, X. Liang, M. Piatko, S. Campbell, S.K. Lo, Y. Liu, Synergetic interfacial adsorption of protein and low-molecular-weight emulsifiers in aerated emulsions, Food Hydrocoll. 81 (2018) 15–22. doi:10.1016/j.foodhyd.2018.02.038.

[13] B.A. Noskov, M.M. Krycki, Formation of protein/surfactant adsorption layer as studied by dilational surface rheology, Adv. Colloid Interface Sci. 247 (2017) 81–99. doi:10.1016/j.cis.2017.07.003.

[14] M. Ishtikhar, M.S. Ali, A.M. Atta, H.A. Al-Lohedan, L. Nigam, N. Subbarao, R. Hasan Khan, Interaction of biocompatible natural rosin-based surfactants with human serum albumin: A biophysical study, J. Lumin. 167 (2015) 399–407. doi:10.1016/j.jlumin.2015.06.012.

[15] C. Berton, C. Genot, M.H. Ropers, Quantification of unadsorbed protein and surfactant emulsifiers in oil-in-water emulsions, J. Colloid Interface Sci. 354 (2011) 739–748. doi:10.1016/j.jcis.2010.11.055.

[16] Y. Liang, L. Matia-Merino, G. Gillies, H. Patel, A. Ye, M. Golding, The heat stability of milk protein-stabilized oil-in-water emulsions: A review, Curr. Opin. Colloid Interface Sci. 28 (2017) 63–73. doi:10.1016/j.cocis.2017.03.007.

[17] S. Kerstens, B.S. Murray, E. Dickinson, Microstructure of β-lactoglobulin-stabilized emulsions containing non-ionic surfactant and excess free protein: Influence of heating, J. Colloid Interface Sci. 296 (2006) 332–341. doi:10.1016/j.jcis.2005.08.046.

[18] W. Aehle, Enzymes in Industry Production and Applications, Wiley-VCH, 2007.

[19] M.A. James-Smith, B. Hellner, N. Annunziato, S. Mitragotri, Effect of surfactant mixtures on skin structure and barrier properties, Ann. Biomed. Eng. 39 (2011) 1215–1223. doi:10.1007/s10439-010-0190-4.

[20] S. Ghosh, D. Blankschtein, The role of sodium dodecyl sulfate (SDS) micelles in inducing skin barrier perturbation in the presence of glycerol, J. Cosmet. Sci. 58 (2007) 109–133. doi:10.1111/j.1468-2494.2007.00401_1.x.

[21] Z. Draelos, S. Hornby, R.M. Walters, Y. Appa, Hydrophobically modified polymers can minimize skin irritation potential caused by surfactant-based cleansers, 2013.

[22] F. Hasan, A. Shah, S. Javed, A. Hameed, Enzymes used in detergents: Lipases, African J. Biotechnol. 9 (2010) 4836–4844. doi:10.5897/AJBx09.026.

[23] B. Jonsson, B. Lindman, K. Holmberg, Surfactants and polymers in aqueous solutions, IEEE Electr. Insul. Mag. 14 (1998) 42–43. doi:10.1109/MEI.1998.714652.

[24] B.S. Chang, S. Hershenson, Practical Approaches to Protein Formulation Development, in: 2002: pp. 1–25. doi:10.1007/978-1-4615-0557-0_1.

[25] E.O. Stejskal, J.E. Tanner, Spin diffusion measurements: Spin echoes in the presence of a time-dependent field gradient, J. Chem. Phys. 42 (1965) 288–292. doi:10.1063/1.1695690.

[26] J.M. Berg, J.L. Tymoczko, L. Stryer, Biochemistry, 5th ed., W. H. Freeman, New York, 2002.

[27] G.A. Picó, Thermodynamic features of the thermal unfolding of human serum albumin, Int. J. Biol. Macromol. 20 (1997) 63–73. doi:10.1016/S0141-8130(96)01153-1.

[28] M.R. Eftink, The use of fluorescence methods to monitor unfolding transitions in proteins, Biophys. J. 66 (1998) 482–501.

[29] L. Zhao, R. Liu, X. Zhao, B. Yang, C. Gao, X. Hao, Y. Wu, New strategy for the evaluation of CdTe quantum dot toxicity targeted to bovine serum albumin, (2009). doi:10.1016/j.scitotenv.2009.05.052.

[30] S. Chakraborti, P. Joshi, D. Chakravarty, V. Shanker, Z.A. Ansari, S.P. Singh, P. Chakrabarti, Interaction of Polyethyleneimine-Functionalized ZnO Nanoparticles with Bovine Serum Albumin, 28 (2012) 31. doi:10.1021/la3007603.

[31] A.J. Rader, B.M. Hespenheide, L.A. Kuh, M.F. Thorpe, Protein unfolding: Rigidity lost, Proc. Natl. Acad. Sci. U. S. A. 99 (2002) 3540–3545. doi:10.1073/pnas.062492699.

[32] G. Palazzo, F. Lopez, A. Mallardi, Effect of detergent concentration on the thermal stability of a membrane protein: The case study of bacterial reaction center solubilized by N,N-dimethyldodecylamine-N-oxide, Biochim. Biophys. Acta - Proteins Proteomics. 1804 (2010) 137–146. doi:10.1016/j.bbapap.2009.09.021.

[33] T. Janek, Czyżnikowska, J. Łuczyński, E.J. Gudiña, L.R. Rodrigues, J. Gałęzowska, Z. Czy, J. Łuczy´nski, Ł. Łuczy´nski, E.J. Gudiña, G. Gudiña, L.R. Rodrigues, J. Gał, ˛ Ezowska, J. Burger, J. Łuczy, E.J. Gudi, L.R. Rodrigues, J. Gał, Physicochemical study of biomolecular interactions between lysosomotropic surfactants and bovine serum albumin, Colloids Surfaces B Biointerfaces. 159 (2017) 750–758. doi:10.1016/j.colsurfb.2017.08.046.

[34] V. Sharma, O. Yañez, M. Alegría-Arcos, A. Kumar, R.C. Thakur, P. Cantero-lópez, J.C. Thermodynamics, V. Sharma, O. Yañez, M. Alegría-Arcos, A. Kumar, R.C. Thakur, P. Cantero-lópez, A physicochemical and conformational study of co-solvent effect on the molecular interactions between similarly charged protein surfactant (BSA-SDBS) system, J. Chem. Thermodyn. 142 (2020) 106022. doi:10.1016/j.jct.2019.106022.

[35] E.L. Gelamo, M. Tabak, Spectroscopic studies on the interaction of bovine (BSA) and human (HSA) serum albumins with ionic surfactants, Spectrochim. Acta - Part A. 56 (2000) 2255–2271. doi:1386-1425/00/$.

[36] D.E. Otzen, Proteins in a brave new surfactant world, Curr. Opin. Colloid Interface Sci. 20 (2015) 161–169. doi:10.1016/j.cocis.2015.07.003.

[37] K.K. Andersen, C.L. Oliveira, K.L. Larsen, F.M. Poulsen, T.H. Callisen, P. Westh, J.S. Pedersen, D. Otzen,

The Role of Decorated SDS Micelles in Sub-CMC Protein Denaturation and Association, J. Mol. Biol. 391 (2009) 207–226. doi:10.1016/j.jmb.2009.06.019.

[38] A.D. Nielsen, K. Borch, P. Westh, Thermal Stability of Humicola insolens Cutinase in aqueous SDS, J. Phys. Chem. B. 111 (2007) 2941–2947. doi:10.1021/jp065896u.

[39] T. Janek, Ż. Czy, Ł. Marcin, J. Ga, Ż. Czyżnikowska, M. Łukaszewicz, J. Galęzowska, The effect of Pseudomonas fluorescens biosurfactant pseudofactin II on the conformational changes of bovine serum albumin: Pharmaceutical and biomedical applications, J. Mol. Liq. 288 (2019) 111001. doi:10.1016/j.molliq.2019.111001.

[40] T. Janek, L.R. Rodrigues, E.J. Gudiña, Ż. Czyżnikowska, Z. Czy ˙ Znikowska, Metal-Biosurfactant Complexes Characterization: Binding, Self-Assembly and Interaction with Bovine Serum Albumin, Int. J. Mol. Sci. 20 (2019) 2864. doi:10.3390/ijms20122864.

[41] B.K. Paul, A. Samanta, N. Guchhait, Exploring Hydrophobic Subdomain IIA of the Protein Bovine Serum Albumin in the Native , Intermediate , Unfolded , and Refolded States by a Small Fluorescence Molecular Reporter Exploring Hydrophobic Subdomain IIA of the Protein Bovine Serum Albumin in the, (2019). doi:10.1021/jp100004t.

[42] R. Li, Z. Wu, Y. Wangb, L. Ding, Y. Wang, Role of pH-induced structural change in protein aggregation in foam fractionation of bovine serum albumin, Biotechnol. Reports. 9 (2016) 46–52. doi:10.1016/j.btre.2016.01.002.

[43] A. Papagiannopoulos, Bovine serum albumin interactions with cationic surfactant vesicles decorated by a low-molar-mass polysaccharide, Colloids Surfaces A. 537 (2018) 495–501. doi:10.1016/j.colsurfa.2017.10.058.

[44] P. Stilbs, Fourier transform pulsed-gradient spin-echo studies of molecular diffusion, Prog. Nucl. Magn. Reson. Spectrosc. 19 (1987) 1–45. doi:10.1016/0079-6565(87)80007-9.

[45] A. Chen, D. Wu, C.S.J. Johnson, Determination of the Binding Isotherm and Size of the Bovine Serum Albumin-Sodium Dodecyl Sulfate Complex by Diffusion-Ordered 2D NMR, J. Phys. Chem. 99 (1995) 828–834. doi:10.1021/j100002a054.